

# Inverse and direct magnetoelectric effects in orthorhombic DyMnO<sub>3</sub> manganite single crystals

Cite as: J. Appl. Phys. **128**, 094102 (2020); <https://doi.org/10.1063/5.0006595>

Submitted: 05 March 2020 . Accepted: 17 August 2020 . Published Online: 02 September 2020

A. L. Freidman,  S. V. Semenov, M. I. Kolkov, K. Yu. Terent'ev, N. S. Pavlovskiy,  D. M. Gokhfeld, K. A. Shaykhutdinov, and D. A. Balaev



View Online



Export Citation



CrossMark

## ARTICLES YOU MAY BE INTERESTED IN

[Ferroelectric and dielectric properties of improper ferroelectric Ca<sub>8-x</sub>Sr<sub>x</sub>\[Al<sub>12</sub>O<sub>24</sub>\]\(MoO<sub>4</sub>\)<sub>2</sub> multilayer capacitors](#)

Journal of Applied Physics **128**, 094101 (2020); <https://doi.org/10.1063/5.0016533>

[Evolution of superparamagnetism in the electrochemical dealloying process](#)

Journal of Applied Physics **128**, 093904 (2020); <https://doi.org/10.1063/5.0015397>

[FORC signatures and switching-field distributions of dipolar coupled nanowire-based hysteron](#)

Journal of Applied Physics **128**, 093903 (2020); <https://doi.org/10.1063/5.0020407>



## Your Qubits. Measured.

Meet the next generation of quantum analyzers

- Readout for up to 64 qubits
- Operation at up to 8.5 GHz, mixer-calibration-free
- Signal optimization with minimal latency

Find out more





# Inverse and direct magnetoelectric effects in orthorhombic DyMnO<sub>3</sub> manganite single crystals

Cite as: J. Appl. Phys. 128, 094102 (2020); doi: 10.1063/5.0006595

Submitted: 5 March 2020 · Accepted: 17 August 2020 ·

Published Online: 2 September 2020



A. L. Freidman,<sup>1</sup> S. V. Semenov,<sup>1,2,a)</sup>  M. I. Kolkov,<sup>1</sup> K. Yu. Terent'ev,<sup>1</sup> N. S. Pavlovskiy,<sup>1</sup> D. M. Gokhfeld,<sup>1,2</sup>   
K. A. Shaykhutdinov,<sup>1</sup> and D. A. Balaev<sup>1,2</sup>

## AFFILIATIONS

<sup>1</sup>Kirensky Institute of Physics, Federal Research Center KSC SB RAS, Krasnoyarsk 660036, Russia

<sup>2</sup>Institute of Engineering Physics and Radio Electronics, Siberian Federal University, Krasnoyarsk 660041, Russia

<sup>a)</sup>Author to whom correspondence should be addressed: svsemenov@iph.krasn.ru

## ABSTRACT

Correlations between the direct and inverse magnetoelectric effects in orthorhombic DyMnO<sub>3</sub> single crystals have been investigated. In the inverse magnetoelectric effect, the magnetic moment of the crystal appears to have a contribution that is sinusoidal oscillating in ac electric fields below the temperature  $T_{FE}$  of ferroelectric phase transition. The first and the second harmonics of the inverse magnetoelectric effect are clearly detected. The magnetoelectric susceptibilities  $\alpha$  and  $\beta$ , corresponding to first and second harmonics, are found to correlate with the derivative of polarization with respect to the magnetic field. The influence of the magnetic and electric regimes during cooling on magnetoelectric effects has also been studied. The maximum change in the magnetic moment of a sample under the action of electric fields is observed under the same  $(T, H)$  conditions as the rotation of the spontaneous polarization vector from the crystallographic  $c$  direction to the  $a$  axis in the magnetic field  $H \parallel b$ .

Published under license by AIP Publishing. <https://doi.org/10.1063/5.0006595>

## INTRODUCTION

In recent times, multiferroics belonging to the class of rare-earth RMnO<sub>3</sub> ( $R^{3+}$  is the rare-earth ion) manganites have been intensively investigated.<sup>1–16</sup> One of the most intriguing families of these compounds is the orthorhombic manganites (space group  $Pbnm$ ). Depending on the ionic radius of the rare-earth element, different types of magnetic ordering are established in them. According to the phase diagram presented in Ref. 1, for  $R = La, \dots, Gd$ , the A-type antiferromagnetic (AFM) ordering is observed in the ground state. For small-radii rare-earth ions ( $R = Ho, \dots, Yb, Y, Sc$ ), E-type AFM ordering is established.<sup>2–5</sup> There are improper TbMnO<sub>3</sub> and DyMnO<sub>3</sub> ferroelectrics on the boundary between A-AFM and E-AFM regions of the phase diagram.<sup>6</sup> At low temperatures, a spiral (cycloidal) magnetic structure of the manganese moments forms in these compounds, which is accompanied by ferroelectric ordering.<sup>7</sup>

The detailed study of the temperature evolution of the magnetic structure in the orthorhombic RMnO<sub>3</sub> ( $R = Tb$  and Dy) compounds<sup>7,8</sup> showed that the incommensurate AFM ordering, which represents a sinusoidal modulated collinear structure consisting of only the manganese magnetic moments, is established at temperatures of  $T_N = 39$  K

for Dy and  $T_N = 41$  K for Tb. With a further decrease in temperature to  $T_{FE} = 18$  K for Dy and  $T_{FE} = 28$  K for Tb, transition to the non-centrosymmetric spiral (cycloidal) magnetic structure occurs.<sup>9</sup> The absence of an inversion center and the nonuniform magnetoelectric interaction<sup>10</sup> lead to the occurrence of electric polarization  $\mathbf{P}$ . The value of  $\mathbf{P}$  changes in an applied magnetic field  $H$ , which is the direct magnetoelectric effect.<sup>7,9–11</sup> In addition, the observed electric polarization is sensitive to the direction of an external magnetic field. For example, in the orthorhombic DyMnO<sub>3</sub> crystals, the spontaneous polarization vector changes its direction from  $\mathbf{P} \parallel c$  to  $\mathbf{P} \parallel a$  and then an external magnetic field is applied in the  $ab$  plane.<sup>7</sup> This behavior is apparently related to the rotation of the spin cycloid from the  $bc$  to the  $ab$  plane.<sup>1,9,12</sup> The results obtained are indicative of the strong interplay of the electric and magnetic subsystems, which makes these compounds promising for application.<sup>13</sup> Of fundamental interest is the establishment of mechanisms responsible for the observed magnetoelectric phenomena.<sup>14</sup>

The strong magnetoelectric interaction makes it possible to control the electric polarization by applying an external magnetic field<sup>16</sup> and, vice versa, to affect the magnetic subsystem by applying an electric field.<sup>17</sup> Therefore, the magnetoelectric effect manifests

itself in two ways: (i) a direct magnetoelectric effect is polarization change  $\Delta P$  in the applied magnetic field  $H$ ; (ii) an inverse magnetoelectric effect is magnetization change  $\Delta M$  in the applied electric field  $E$ . The direct effect in the discussed compounds was thoroughly investigated both experimentally<sup>7,8</sup> and theoretically,<sup>1,12,15</sup> whereas only fragmentary studies were devoted to the effect of an electric field on the magnetic subsystem in orthorhombic manganites.<sup>18,19</sup> It may be said that while the direct magnetoelectric effect is a conventional approach to study the coupling of magnetic and electric subsystems in orthorhombic manganites, the inverse effect is unexplored. In the present research, we carried out a detailed experimental study of both the direct and inverse magnetoelectric effects in the orthorhombic  $\text{DyMnO}_3$  single crystals in order to fill the gap and to establish regularities and interplay between direct and inverse magnetoelectric effects.

## EXPERIMENTAL

The  $\text{DyMnO}_3$  single crystals were synthesized by spontaneous crystallization from the flux. Their magnetic properties were reported before.<sup>20</sup> The average sizes of the obtained single crystals were about  $1 \times 1 \times 1.5 \text{ mm}^3$ . According to the x-ray diffraction data, the synthesized  $\text{DyMnO}_3$  single crystals have an orthorhombic space group  $Pbnm$  with lattice parameters  $a = 5.2816 \text{ \AA}$ ,  $b = 5.8457 \text{ \AA}$ , and  $c = 7.3802 \text{ \AA}$ .<sup>20</sup> The specific heat  $C_p(T)$  of the samples was measured on a QD PPMS-9 facility. The magnetization was measured on a home-made vibrating sample magnetometer with a superconducting solenoid.<sup>21</sup>

To measure the direct and inverse magnetoelectric effects, a sample in the form of a flat capacitor was prepared (Fig. 1). The capacitor plates formed from an epoxy-based conductive paste with a silver filler were deposited onto the preliminary polished crystal faces perpendicular to the  $a$  axis.

Electric polarization (the  $\text{ME}_H$  effect) was determined by measuring the electric charge flowing off the capacitor plates with a

Keithley 6517B electrometer. The spontaneous polarization during transition to the ferroelectric state can give rise to a domain structure, in which the charge on the sample surface is partially or fully compensated by the domains with oppositely directed polarization.<sup>22,23</sup> To ensure a single-domain state, the sample was prepolarized before the measurements of the magnetoelectric effect. The electric field was applied to the opposite sample faces at a temperature above  $T_{FE}$ ; the sample was cooled in the applied electric field. After that, the applied electric field was switched off and the measurements started.

The spontaneous polarization vector  $\mathbf{P}$  along the  $c$  direction can be directed oppositely by an external electric field. Also, in the orthorhombic  $\text{DyMnO}_3$  crystals, the polarization vector can be flopped to the  $a$  direction by an external magnetic field applied in the  $ab$  plane.<sup>7</sup> To study the polarization behavior in this compound, it is necessary to take into account a prehistory, which includes cooling in both an electric field and a magnetic field. Therefore, the measurements were performed also upon cooling in a magnetic field. Before the measurements, the sample was prepolarized by cooling in a dc electric field  $E_0 = 7.4 \text{ kV/cm}$  applied along the  $a$  axis of the crystal and in different magnetic fields  $H$  applied along the  $b$  axis to the temperatures below  $T_{FE}$ . After that, the external field was switched off and the measurements started. The specific polarization of the unit volume was determined as  $P = Q/S$ , where  $Q$  is the charge that flew off the sample surface with area  $S$ . The temperature and field dependences of polarization  $P_a$  along the  $a$  axis of the crystal were measured. During the polarization measurements, the magnetic field  $H_b$  was applied along the  $b$  direction (here and through all lower indices indicate the direction along the corresponding axes).

The inverse magnetoelectric ( $\text{ME}_E$ ) effect was measured on an original experimental setup using the same sample (Fig. 1). The experimental setup and measurement technique were described in detail in Refs. 24–26. Before the measurements, the sample was prepolarized by cooling in a dc electric field of  $E_0 = 7.4 \text{ kV/cm}$  ( $200 \text{ V}/0.27 \text{ mm}$ ) applied along the  $a$  axis of the crystal. After cooling, the polarizing field was switched off and the ac electric field  $E = E_0 \cdot \cos(\omega t)$  with an amplitude of  $E_0 = 3.7 \text{ kV/cm}$  and a frequency of  $f = \omega/2\pi = 1 \text{ kHz}$  was applied to the capacitor plates. Due to the magnetoelectric effect, the applied ac electric field  $E$  changes the magnetic moment of the sample according to the periodic law. As a result, the voltage is generated in a pickup coil, which is proportional to the amplitude of the magnetic moment oscillations in the sample.

The exciting electric field was only applied along the  $a$  axis, and the magnetic moment change  $\Delta M$  along the  $b$  axis (the transverse  $\text{ME}_E$  effect) was detected. The signal was measured by an SR830 lock-in amplifier, which determines the first and second harmonics ( $\Delta M'$  and  $\Delta M''$ ) of the magnetic moment oscillations. The first harmonic corresponds to the magnetic moment oscillations at the frequency  $\omega$  of the exciting electric field and the second to the magnetic moment oscillations at the doubled frequency  $2\omega$ . The harmonics are determined as  $\Delta M' = \alpha \cdot E_0$  and  $\Delta M'' = \beta \cdot E_0^2$ ,<sup>26</sup> where  $\alpha$  and  $\beta$  are the susceptibilities of the first and second harmonics of the inverse magnetoelectric effect by the electric field and  $E_0$  is the oscillation amplitude of the applied electric field.

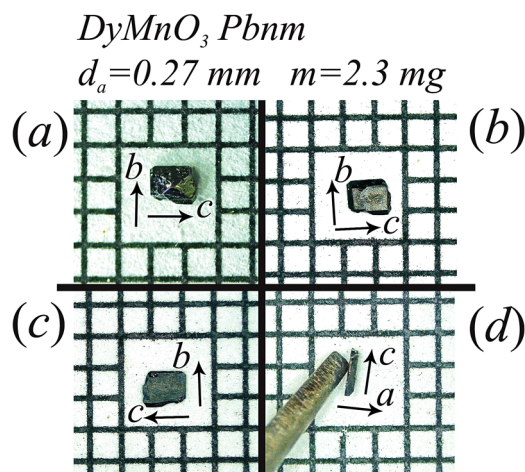


FIG. 1. Sample for investigations before (a) and after [(b)(d)] the mechanical treatment. The grid step equals 1 mm.

RESULTS AND DISCUSSION

The temperature dependence of specific heat for the sample under study is shown in Fig. 2 (in the right-hand axis). With the temperature decreasing, three pronounced features arise in  $C_p(T)$  dependence, which are related to magnetic transitions in  $\text{DyMnO}_3$ .<sup>7</sup> The kink in the curve at  $T = 40$  K corresponds to the occurrence of the AFM ordering in the manganese subsystem. The peak at  $T_{FE} \sim 18$  K is related to the transition of the manganese subsystem from the sinusoidal modulated collinear magnetic structure to spiral (cyclodial) one. This transition is accompanied by ferroelectric ordering. Finally, the dysprosium subsystem is ordered at a temperature of  $T \sim 8$  K. It is worth noting that the first two features (at  $T = 40$  and 18 K) are not seen on the temperature dependence of magnetization  $M_b(T)$  (the left-hand axis in Fig. 2) due to the great paramagnetic contribution of dysprosium ions.<sup>20</sup>

Figure 3 shows temperature dependences of polarization  $P_a$  of the  $\text{DyMnO}_3$  single crystal in different magnetic fields. Before each measurement, the sample was warmed up to 100 K; then an electric field of 7.4 kV/cm was applied along the  $a$  direction and the sample was cooled down to  $T = 4.2$  K; after that, the electric field was switched off, a magnetic field was applied, and the  $P(T, H_b)$  measurements were performed. It is seen in Fig. 3 that, under these experimental conditions, the polarization is low and does not exceed  $150 \mu\text{C}/\text{m}^2$  even in the lowest temperatures; in addition, one can see that the polarization is almost absent at temperatures above  $T_{FE} \sim 18$  K.

Upon cooling to  $T_{FE}$ , the spontaneous electric polarization along the  $c$  axis occurs [case (i) in Fig. 4]. The electric field applied along the  $a$  axis does not significantly affect the domain structure of a ferroelectric [case (iii) in Fig. 4]. After switching-off the electric field  $E_a$  and applying the magnetic field  $H_b$  of above 20 kOe (at  $T = 4.2$  K), the polarization switches from  $c$  to  $a$  direction ( $P_c \rightarrow P_a$ ). However, since the external electric field is not applied in this case, the ferroelectric can be arbitrary divided into domains [case (ii) in Fig. 4]. The dependences measured in magnetic fields of 10 and

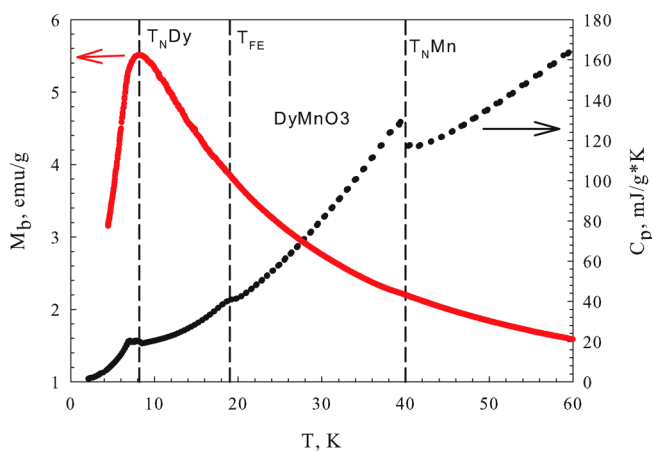


FIG. 2. Temperature dependences of magnetization  $M_b(T)$  (left-hand axis) at  $H = 1$  kOe ( $H \parallel b$ ) and specific heat  $C_p(T)$  (right-hand axis) at  $H = 0$ .

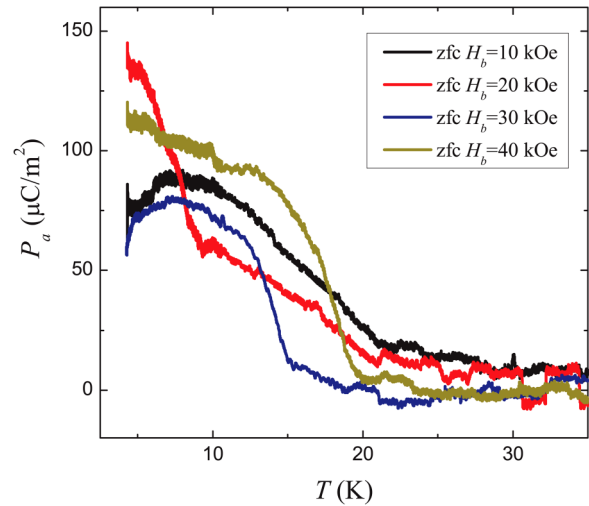


FIG. 3. Temperature dependences of electric polarization  $P_a$  along the  $a$  direction in different magnetic fields  $H_b$  applied along the  $b$  axis. Before each measurement, the sample was cooled from 100 K to 4.2 K in  $E_a = 7.4$  kV/cm and  $H = 0$ . The measurements were performed in a warming mode.

40 kOe correspond to two spontaneous polarization directions  $\mathbf{P} \parallel c$  and  $\mathbf{P} \parallel a$ , respectively (Fig. 3). It can be seen that there is no significant difference between these dependencies. It implies that polarization  $P_a$  induced in the magnetic field  $H_b$  is compensated by the domain structure.

An absolutely different case occurs when the sample is cooled in the simultaneously applied electric field  $E_a$  and magnetic field  $H_b$ . Figure 5(a) shows temperature dependences of polarization  $P_a(T, H_b)$ . The measurements were performed in the following manner: at a temperature of 100 K, the electric field  $E_a$  and magnetic field  $H_b$  were applied, and the sample was cooled down to 4.2 K; then, the electric field was switched off and the polarization measurements started in the sample warming up regime, while the magnetic field remained invariable.

It can be seen in Fig. 5(a) that the polarization obtained after cooling in the magnetic field of 10 kOe is comparable in an order

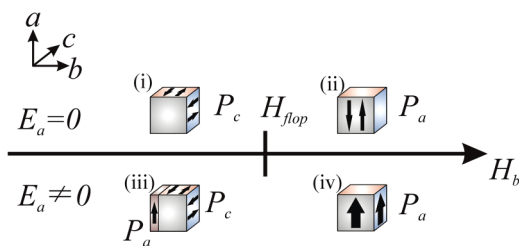
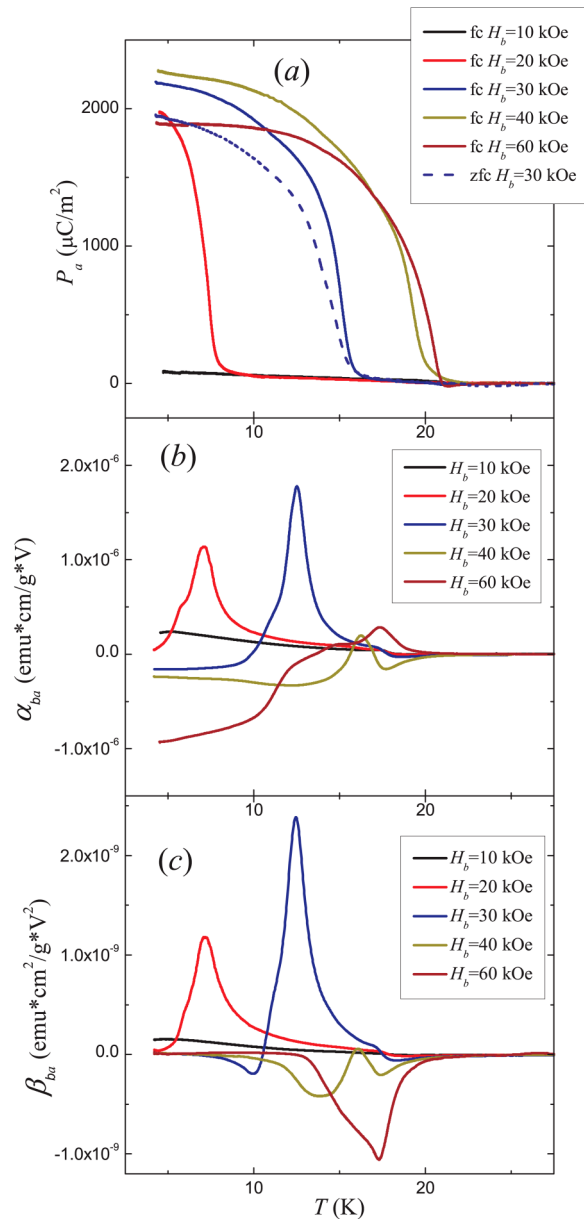


FIG. 4. Scheme of the ferroelectric domain structure in applied electric and magnetic fields. The magnetic field  $H_{flop}$  corresponds to polarization vector switching.



**FIG. 5.** Temperature dependences of the electric polarization  $P_a$  (a) and susceptibility of the first  $\alpha_{ba}$  and second  $\beta_{ba}$  harmonics of the  $ME_E$  effect [(b) and (c)] in different magnetic fields  $H_b$ . The measurements were performed in a warming mode.

of magnitude with the results obtained after cooling in a zero magnetic field (Fig. 3); this corresponds to case (iii) in Fig. 4; the latter implies that the value of  $H_b = 10$  kOe is insufficient to upset the polarization vector to the  $a$  direction, at least, in the investigated temperature range, which is consistent with the results obtained in Ref. 7. However, upon cooling in a field of 20 kOe and more, one

can observe a sharp increase in polarization [case (iv) in Fig. 4]: at low temperatures, it is more than  $2000 \mu\text{C}/\text{m}^2$ . The polarization switching field  $H_{flop}$  depends on the temperature. The steep polarization drop with increasing temperature is related to the inverse switching of the vector:  $P_a \rightarrow P_c$ ; in this case, the higher field  $H_b$  corresponds to the higher temperature of flop transition. In sufficiently strong magnetic fields  $H_b$  (40 kOe and more), the polarization  $P_a$  vanishes at temperature  $T_{FE}$  on transition to the paraelectric state.

The dashed curve in Fig. 5(a) is worth to be described separately. This curve was obtained after cooling the sample from 100 K in zero electric and magnetic fields:  $E = 0$  and  $H = 0$ . In contrast to zero-field cooled (ZFC) dependences in Fig. 3, both an electric field of  $E_a = 7.4$  kV/cm and a magnetic field of  $H_b = 30$  kOe were applied at  $T = 4.2$  K. Then, the electric field was switched off and the temperature dependence of polarization was measured. Thus, at low temperature, the polarization vector switching  $P_c \rightarrow P_a$  was induced by the magnetic field, and the electric field led to the predominance of one direction in the domain structure of the crystal [case (iv) in Fig. 4]. However, it can be seen in Fig. 5(a) that the polarization obtained after such a prehistory is somewhat lower than the polarization after cooling from high temperatures in the electric and magnetic fields with the same values ( $H_b = 30$  kOe and  $E_a = 7.4$  kV/cm).

Figures 5(b) and 5(c) show temperature dependences of magnetoelectric susceptibility of the first ( $\alpha_{ba}$ ) and second ( $\beta_{ba}$ ) harmonics of the  $ME_E$  effect, respectively. These data were obtained in the configuration with the magnetic field applied along the  $b$  axis, the electric field applied along the  $a$  axis, and the magnetic moment change detected along the  $b$  axis.

Our measurements in the zero magnetic field ( $H = 0$ ) showed that the  $ME_E$  effect is absent, i.e., under the action of an ac electric field, the oscillations of the magnetic moment relative to zero are not observed:  $\Delta M' = 0$  ( $\alpha = \beta = 0$ ). However, in a dc magnetic field, when the sample has a certain constant magnetic moment, we observe the oscillations of this moment  $\Delta M' \neq 0$  ( $\alpha \neq 0$ ), which are excited by an ac electric field. This behavior corresponds to the nonlinear magnetoelectric effect.<sup>27</sup>

The inverse  $ME_E$  effect has a maximum, which shifts toward higher temperatures with the increasing magnetic field. This reflects the behavior of polarization. Indeed, it can easily be seen from the comparison of  $P_a(T)$ ,  $\alpha_{ba}(T)$ , and  $\beta_{ba}(T)$  dependences that, in this magnetic field, the  $\alpha_{ba}(T)$  and  $\beta_{ba}(T)$  peaks lie in the same temperature region as the  $P_a(T)$  inflection points. In addition, it can be seen that the magnetoelectric effect vanishes after approaching a temperature of  $T_{FE} \sim 18$  K. However, the magnetic field  $H_b$  of more than 30 kOe somewhat increases this temperature; the similar shift of temperature  $T_{FE}$  in strong magnetic fields is observed also for polarization.

Figure 6(a) shows field dependences of polarization  $P_a(H_b)$  at  $T = 4.2$  K obtained for different sample prehistories. The black curve shows the dependence of polarization of the sample frozen in the electric field  $E_a$  without a magnetic field. It can be seen that, in this case, a two-step polarization jump occurs near 10 and 20 kOe. This jump is caused by polarization vector switching  $P_c \rightarrow P_a$ . However, since the polarizing electric field is already switched off, the transition to the multi-domain state occurs and the resulting polarization is low.

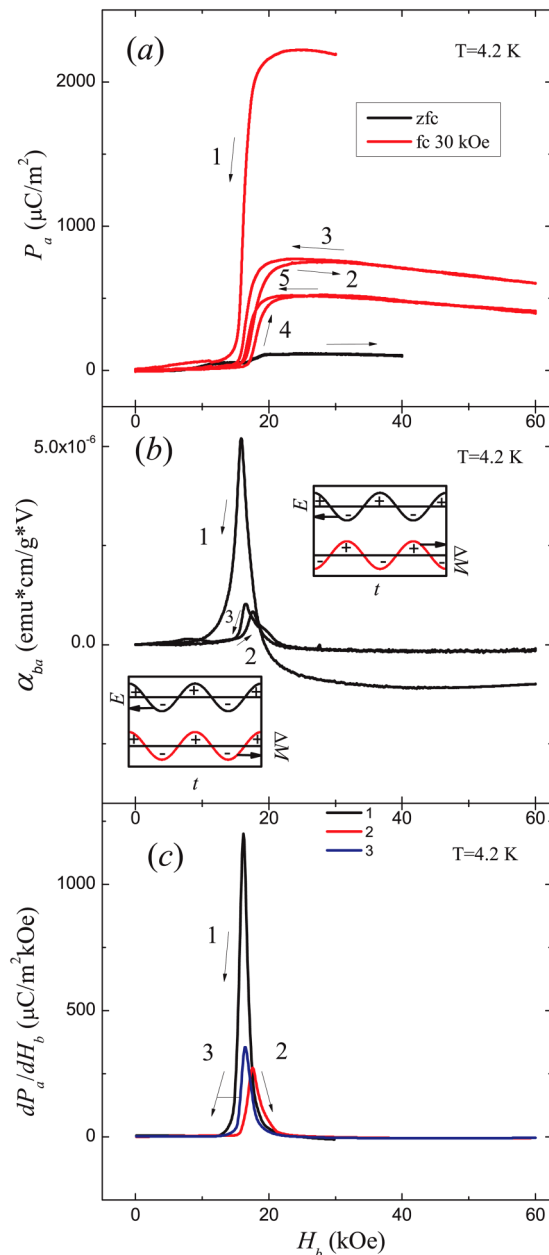


**FIG. 6.** Field dependences of the electric polarization  $P_a(H)$  (a) and the susceptibility of the first harmonic of the  $\text{ME}_E$  effect  $\alpha_{ba}(H)$  (b) and the first magnetic field derivative  $dP_a/dH_b$  (c) at the temperature of 4.2 K. The insets in b show the  $\Delta M(t)$  behavior before and after passing the point of the change in the sign of the  $\text{ME}_E$  effect.

The red curve was obtained after cooling the sample from 100 K to 4.2 K in the polarizing electric field  $E_a$  and a magnetic field of  $H_b = 30$  kOe; it can be seen that, in this case, the polarization values are much higher. Before the measurements, the electric

field was switched off and the course of polarization [shown by arrow 1 in Fig. 6(a)] was recorded; a decrease in polarization is related to the polarization vector switching  $P_a \rightarrow P_c$ . If we apply a magnetic field again and induce transition  $P_c \rightarrow P_a$  (the curve shown by arrow 2), then polarization  $P_a$  does not attain its initial value, since in this case, the polarizing electric field  $E_a$  is not applied during transition and the domain structure arises. Nevertheless, this polarization is much higher than that in the ZFC case; it means that the crystal keeps the memory about the preferred direction of polarization  $P_a$  even after the return to the state  $P_c$ . However, the greater number of magnetic field cycles inducing sequential transitions  $P_a \rightarrow P_c \rightarrow P_a$  corresponds to lower resulting polarization  $P_a$ . Figure 6(a) shows also that polarization switching has a magnetic hysteresis.

Analogously to the above-described polarization measurements, we measured the magneto-electric susceptibility  $\alpha_{ba}(H_b)$  after cooling in the electric field  $E_0$  and the magnetic field of  $H_b = 60$  kOe [Fig. 6(b)]. The initial course of the curve corresponds to a decrease in the magnetic field from 60 kOe to 0 kOe (shown by black arrow 1). With a further increase and decrease in the magnetic field  $H_b$  (the curves are shown by arrows 2 and 3, respectively), the peak of magneto-electric susceptibility decreases. Similar to polarization, the inverse magneto-electric effect has a magnetic field hysteresis. In addition, in strong magnetic fields, the susceptibility  $\alpha_{ba}$  becomes negative.

The  $\text{ME}_E$  effect and  $\Delta M$  change the sign at the same electric field. Strictly speaking, the electric field direction does not affect an increase or a decrease in the magnetic moment. This direction is apparently related to the direction of the prepolarizing field  $E_0$ . However, during the measurements, while the magnetic field increases, the signal phase  $\Delta M(t)$  was detected to shift by  $\pi$ . The insets in Fig. 6(b) show the  $\Delta M(t)$  behavior before and after passing the point of the sign change of the  $\text{ME}_E$  effect. Here, we should note that the magneto-electric susceptibility is negative in the magnetic field region where the  $P_a(H_b)$  curve has a negative slope (Fig. 6).

To trace the correlation between the direct and inverse magneto-electric effects, we presented the derivative  $dP_a/dH_b$ , which is conventionally named as the linear susceptibility of the direct  $\text{ME}_H$  effect to the magnetic field  $H_b$ . The comparison of Figs. 6(b) and 6(c) shows that the curves are very similar. The derivative  $dP_a/dH_b$  becomes negative in field of above 20 kOe. However, the negative course is much less pronounced than in the  $\alpha_{ba}(H_b)$  dependence.

The field dependences of the susceptibility of the  $\text{ME}_E$  effect at different temperatures are presented in Fig. 7. These dependences were measured after cooling the sample in the dc electric field  $E_0$  without a magnetic field. As can be seen from the comparison of the plots in Figs. 6(b) and 7, the magneto-electric susceptibility upon cooling in the magnetic and electric fields is several times higher than the value obtained after cooling in only the electric field  $E_0$ . The magneto-electric effect exhibits a magnetic field hysteresis related to polarization switching hysteresis  $P_a \rightarrow P_c \rightarrow P_a$ . Interestingly, the hysteresis of the second harmonic of the  $\text{ME}_E$  effect  $\beta_{ba}(H)$  [Fig. 7(b)] is significantly stronger than the first harmonic hysteresis  $\alpha_{ba}(H)$  and polarization  $P_a(H)$ .

We should pay attention to the fact that, during cooling in the electric field  $E_0$  at temperature  $T_{FE}$ , the spontaneous polarization in

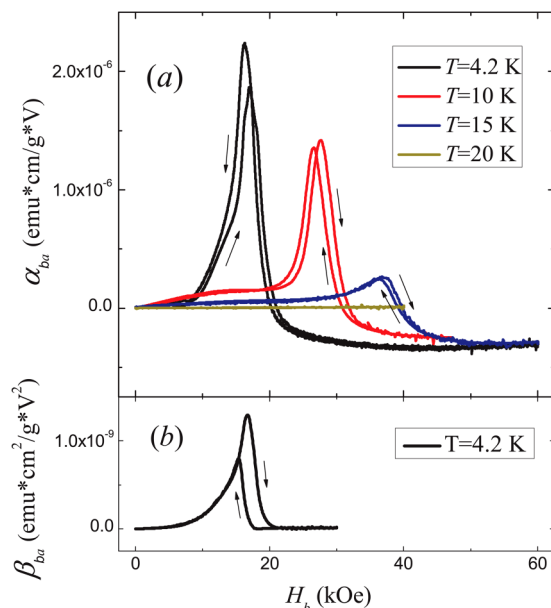


FIG. 7. Field dependences of the  $ME_E$  effect  $\alpha_{ba}(H)$  (a) and  $\beta_{ba}(H)$  (b).

the sample occurs along the  $c$  direction, while the polarizing field  $E_0$  is applied in the orthogonal  $a$  direction. Nevertheless, the magnetoelectric response after such prehistory is nonzero.

In addition, we should keep it in mind that, during  $ME_E$  measurements, a significantly high exciting ac electric field ( $E_0 \sim 3.7$  kV/cm) was applied to the sample; this field was twice as low as the prepolarizing field  $E_0$ ; nevertheless, their values are comparable. Thus, we can expect that the ac electric field with the frequency of 1 kHz makes the sample to be single-domain during the measurements. The used value of  $E_0 \sim 3.7$  kV/cm looks to be sufficient to cause the nonlinear effects related to the polarization hysteresis. In Ref. 7, a ferroelectric loop was observed at the liquid helium temperature in the magnetic field of  $H_b = 60$  kOe and the electric field range of  $\pm 25$  kV/cm. The amplitude  $E_0$  and the frequency  $\omega$  of the exciting electric field should affect the susceptibility of the inverse magnetoelectric effect.

## CONCLUSIONS

The inverse magnetoelectric effect in the orthorhombic  $DyMnO_3$  single crystal was investigated first in wide temperature and magnetic field ranges for the transverse ( $E \parallel a, H \parallel b$ ) configuration. The effect manifests itself after cooling the sample in an external electric field, i.e., after the prepolarization of the sample. The inverse magnetoelectric effect arises in the ferroelectric phase and vanishes above temperature  $T_{FE}$  of phase transition. The analysis of the experimental data with regard to the measured polarization values (the direct magnetoelectric effect) showed that the temperature and field behavior of susceptibility of the inverse magnetoelectric effect correlates with the behavior of polarization. The maximum change in the magnetic moment of the sample under the action of the electric field is

observed under the same temperature and magnetic field ranges as the rotation of the spontaneous polarization vector from the  $c$  crystallographic direction to the  $a$  axis. The direct and inverse magnetoelectric effects in the  $DyMnO_3$  orthorhombic crystals appear to be the two sides of the same coin: the polarization rotation is related to the rotation of the spin cycloid from the  $bc$  to the  $ab$  plane;<sup>9</sup> the inverse magnetoelectric effect is caused by the change in the direction of spin rotation in the cycloid plane in the ac electric field.<sup>19</sup>

## ACKNOWLEDGMENTS

The reported study was funded by Russian Foundation for Basic Research, Government of Krasnoyarsk Territory, Krasnoyarsk Regional Fund of Science to the research project “Research, synthesis and investigation of new oxide single crystals showing the interrelation of magnetic, magnetoelastic and magnetoelectric properties” (Project No. 18-42-243024). The measurements were performed in part on the equipment at the Krasnoyarsk Territorial Center for Collective Use, Krasnoyarsk Scientific Center, Siberian Branch, Russian Academy of Sciences.

## DATA AVAILABILITY

The data that support the findings of this study are available from the corresponding author upon reasonable request.

## REFERENCES

- M. Mochizuki and N. Furukawa, *Phys. Rev. B* **80**, 134416 (2009).
- Y. H. Huang, H. Fjellvåg, M. Karppinen, B. C. Hauback, H. Yamauchi, and J. B. Goodenough, *Chem. Mater.* **18**, 2130 (2006).
- S. Mukherjee, A. Dönni, T. Nakajima, S. Mitsuda, M. Tachibana, H. Kitazawa, V. Pomjakushin, L. Keller, C. Niedermayer, A. Scaramucci, and M. Kenzelmann, *Phys. Rev. B* **95**, 104412 (2017).
- H. Okamoto, N. Imamura, B. C. Hauback, M. Karppinen, H. Yamauchi, and H. Fjellvåg, *Solid State Commun.* **146**, 152 (2008).
- N. Lee, Y. J. Choi, M. Ramazanoglu, W. Ratcliff II, V. Kiryukhin, and S.-W. Cheong, *Phys. Rev. B* **84**, 020101 (2011).
- A. P. Levanyuk and D. G. Sannikov, *Phys. Usp.* **17**, 199 (1974).
- T. Kimura, G. Lawes, T. Goto, Y. Tokura, and A. P. Ramirez, *Phys. Rev. B* **71**, 224425 (2005).
- R. Feyerherm, E. Dudzik, N. Aliouane, and D. N. Argyriou, *Phys. Rev. B* **73**, 180401 (2006).
- T. Kimura and Y. Tokura, *J. Phys. Condens. Matter* **20**, 434204 (2008).
- A. K. Zvezdin and A. P. Pyatakov, *Phys. Usp.* **47**, 416 (2004).
- T. Kimura, T. Goto, H. Shintani, K. Ishizaka, T. Arima, and Y. Tokura, *Nature* **426**, 55 (2003).
- M. Mochizuki and N. Furukawa, *Phys. Rev. Lett.* **105**, 187601 (2010).
- S. Fusil, V. Garcia, A. Barthélémy, and M. Bibes, *Annu. Rev. Mater. Res.* **44**, 91 (2014).
- D. Khomskii, *Physics* **2**, 20 (2009).
- M. Mostovoy, *Phys. Rev. Lett.* **96**, 067601 (2006).
- N. Abe, K. Taniguchi, H. Umetsu, S. Ohtani, and T. Arima, *J. Phys. Conf. Ser.* **200**, 012001 (2010).
- A. L. Freidman, A. D. Balaev, A. A. Dubrovskii, E. V. Eremin, K. A. Shaikhutdinov, V. L. Temerov, and I. A. Gudim, *Phys. Solid State* **57**, 1357 (2015).
- E. V. Milov, A. M. Kadomtseva, G. P. Vorob'ev, Y. F. Popov, V. Y. Ivanov, A. A. Mukhin, and A. M. Balbashov, *JETP Lett.* **85**, 503 (2007).
- Y. Yamasaki, H. Sagayama, T. Goto, M. Matsuura, K. Hirota, T. Arima, and Y. Tokura, *Phys. Rev. Lett.* **98**, 147204 (2007).

- <sup>20</sup>S. V. Semenov, M. I. Kolkov, K. Y. Terent'ev, N. S. Pavlovskiy, M. S. Pavlovskiy, A. D. Vasiliev, A. V. Shabanov, K. A. Shaykhtudinov, and D. A. Balaev, *J. Supercond. Novel Magn.* **32**, 3315 (2019).
- <sup>21</sup>A. D. Balaev, Y. V. Boyarshinov, M. M. Karpenko, and B. P. Khrustalev, *Prib. Tekh. Eksp.* **3**, 167 (1985).
- <sup>22</sup>P. Chu, D. P. Chen, and J.-M. Liu, *Appl. Phys. Lett.* **101**, 042908 (2012).
- <sup>23</sup>A. M. Kadomtseva, Y. F. Popov, G. P. Vorob'ev, K. I. Kamilov, A. P. Pyatakov, V. Y. Ivanov, A. A. Mukhin, and A. M. Balbashov, *J. Exp. Theor. Phys. Lett.* **81**, 19 (2005).
- <sup>24</sup>A. D. Balaev and A. L. Freydmann, *J. Surf. Invest. X-Ray Synchrotron Neutron Tech.* **8**, 17 (2014).
- <sup>25</sup>A. L. Freydmann, A. D. Balaev, A. A. Dubrovskiy, E. V. Eremin, V. L. Temerov, and I. A. Gudim, *J. Appl. Phys.* **115**, 174103 (2014).
- <sup>26</sup>A. L. Freydmann, D. A. Erofeev, V. L. Temerov, and I. A. Gudim, *J. Appl. Phys.* **124**, 134101 (2018).
- <sup>27</sup>H. Schmid, in *Introduction to Complex Mediums for Optics and Electromagnetics*, edited by W. S. Wiegelhofer and A. Lakhtakia (SPIE Press, Bellingham, WA, 2003), p. 176.